ELSEVIER

International Journal of Mass Spectrometry 177 (1998) 111–118

International Journal of Mass Spectrometry

Angular distribution of the ejecta in matrix-assisted laser desorption/ionization: Model dependence

R.E. Johnson[a,*], Y. LeBeyec[b]

[a]*Engineering Physics, University of Virginia, Charlottesville, VA 22903, USA*
[b]*Institut de Physique Nucleaire, CNRS-IN2P3, 91406 Orsay Cedex, France*

Received 24 March 1998; accepted May 28, 1998

Abstract

The angular distribution of the ejecta in matrix-assisted laser desorption/ionization (MALDI) was found to peak back toward the direction of illumination in the experiments of Aksouh et al. [Rapid Commun. Mass Spectrom. 9 (1995) 515]. It is shown here that such a result can be caused by a sample that is made up of crystallites with faces having a distribution of orientations relative to the substrate. The averaging of the yield over such a sample also affects the incident angle and threshold dependence of the yield, and it is shown that the results of Aksouh et al. can help differentiate between proposed models for MALDI. (Int J Mass Spectrom 177 (1998) 111–118) © 1998 Elsevier Science B.V.

Keywords: Desorption; MALDI; Laser

Introduction

Matrix-assisted laser desorption/ionization (MALDI) has proved to be a useful tool for ejecting large, whole biomolecules into the gas phase. This process has enhanced the use of mass spectrometry in molecular biology [1]. Although many aspects of the physics of the desorption/ionization process are roughly understood, there is still debate on the details of the mechanisms for ejection (ablation) and ionization. In a recent review of models, Johnson [2] suggested that models for ablation could be differentiated by measuring the incident angle dependence of the yield produced from a well characterized surface. For instance, in one model the yield per laser pulse is independent of the incident angle. This is the case because the area of irradiation increases with increasing angle whereas the penetration depth of the radiation decreases so that the surface energy density is independent of the incident angle. In other models the yield depends on the cosine of the angle to the surface normal because a transport length determines the depth distribution of energy at the time of ablation. Here, it is shown that the angular distribution of the *ejecta* is also affected by the incident angle dependence of the yield *if* the sample has a distribution in the orientations of crystal faces.

At fluences close to the ion threshold fluence, Aksouh et al. [3] found a directional dependence in the ejected ions that correlated with the incident laser-beam direction. They found that ejection peaked in a direction that was back towards the beam rather than, for instance, normal to the substrate. Such

* Corresponding author.

PII S1387-3806(98)14058-7

effects have been seen in ion-induced ejection due to momentum transfer [4] and to track formation [5]. Aksouk et al. [3] attributed this effect to the shape of the crater produced in the ablation process. By using a single crystal sample, Bogelmann et al. [6] also found a directional dependence for the ejecta and drew the same conclusion. In the latter experiments 500 shots were used, so they may indeed have created a crater with a depth not negligible compared to its width. Recently, Fournier et al. (1997) mapped the crater produced with a large number of shots on two different crystal faces and found the results to be roughly independent of the crystal face. They also found that the crater evolved so that it had a face whose normal pointed back roughly parallel to the beam direction, which is discussed later.

Although craters clearly form due to a large number of shots, it is unlikely that a crater with a depth comparable to the width was created in [3]. The experiments were run very close to the minimum laser fluence that produced observable signal, often called the threshold fluence, and involved only a few shots onto each region of the sample that was not a single crystal. Therefore, although a crater wall effect could be important in some experiments, here we examine an alternative explanation for the results of Aksouh et al. [3]. This explanation is based on the fact that samples formed from vacuum drying of a liquid drop are a distribution of microcrystals *and* the principal ejection direction in ablation is normal to the local surface. In such a situation the ejecta can be emitted, preferentially, back toward the direction of illumination. In light reflection the comparable result is that specular reflection always occurs from a rough surface, causing it to be bright, as there is always a microsurface with the correct orientation.

Irradiation of a faceted surface

The standard MALDI sample, formed by condensing the matrix and analyte from a solution and drying it in a vacuum, is a distribution of small crystals that we will refer to as microcrystalline. The crystal faces in such samples have a distribution of orientations [7]. This distribution can be characterized by the quantity $f(\theta_n)$ that gives the distribution of surfaces of individual microcrystals having their normal directions titled at an angle θ_n to the *substrate normal*. This distribution should be constructed such that the projection of the surface areas onto the substrate, $f(\theta_n)$ cos θ_n, gives the fraction of the substrate covered by crystals. For a substrate that is fully covered with sample,

$$\int_0^1 \int_0^{\pi} f(\theta_n) \cos\theta_n \, d\cos\theta_n \, d\phi = 1 \tag{1}$$

where ϕ is the azimuthal angle. In practice the substrate may not be fully covered, in which case the integral in Eq. (1) is equal to the fractional coverage, 1-f_{ex}, where f_{ex}, is the fraction of the substrate exposed. Finally, integrating $f(\theta_n)$ itself over solid angle gives the increase in actual surface area.

If the surface is illuminated by the laser in a direction normal to the substrate, then $f(\theta_n)$ above can be used to calculate the distribution in illumination angles for the microcrystals. Because the laser is often incident on the sample in a direction other than normal to the substrate, the distribution in the illumination angles changes. We define the angle of incidence to the substrate normal as θ_p and make the assumption that $f(\theta_n)$ can be used in a simple way to obtain the new surface illumination properties. If none of the faces of the microcrystals are shadowed when looking in the direction *normal* to the substrate, then the fraction of the beam that strikes a surface at an illumination angle θ_i is shown in the Appendix to be

$$f(\theta_p, \theta_i) = \frac{1}{\cos\theta_p} f(\theta_n) \cos\theta_i \, \Theta(\cos\theta_i) \times [(1 - P_s)(\theta_n, \theta_p)]$$

$$\Theta(x) = 1; \; x > 0 \tag{2}$$

$$= 0; \; x < 0$$

For a given illumination angle the step function, Θ, accounts for those surfaces that are not exposed because of their orientation and P_s is the probability that surfaces of a particular orientation are in the

shadow of other surfaces. The cosine of the illumination angle for an exposed facet is

$$\cos\theta_i = [\cos\theta_p \cos\theta_n + \sin\theta_p \sin\theta_n \cos\phi] > 0. \quad (3)$$

For a fully covered substrate the incident irradiation must strike some surface, so that the distribution in Eq. (2) also integrates to one

$$\int_0^1 \int_0^\pi f(\theta_p, \theta_i) d\cos\theta_n \, d\phi = 1 \quad (4)$$

If the fraction of ejected molecules intercepting a neighboring surface is small, then measurements of the full ejecta distribution can be used to determine the total yield averaged over a rough or multifaceted surface. Note that the *yield per pulse* in an ablation experiment (unlike the yield per photon in a desorption experiment) includes the increase in substrate area exposed as the illumination direction is tilted. However, each microsurface exposed does not increase in area, rather the number of such surfaces increases, as indicated by the prefactor ($1/\cos\theta_p$) in Eq. (2). Therefore, if the yield for a large flat surface has an incident angle dependence, $Y(\cos\theta_i)$, then the yield averaged over a faceted surface is shown in the Appendix to equal

$$\overline{Y(\theta_p)} = \int_0^1 \int_0^\pi Y(\cos\theta_i) f(\theta_p, \theta_i) \, d\cos\theta_n \, d\phi \quad (5)$$

By using this expression, the angular dependence of measured yields from a multifaceted surface can be tested against models for $Y(\cos\theta_i)$. For instance, Westman et al. [8] studied the incident angle dependence of the total yield for a microcrystalline sample well above the ion threshold fluence.

Unfortunately, the shadowing function in Eq. (2) depends on the details of the surface structure and cannot be given in general. Noting the constraint in Eq. (5), an estimate of the averaged yield is obtained by dropping P_s from $f(\theta_p, \theta_i)$ in Eq. (2) and calling the new function $f'(\theta_p, \theta_i)$. Then

$$\bar{Y} \approx \frac{\int_0^1 \int_0^\pi Y(\cos\theta_i) f'(\theta_p, \theta_i) \, d\cos\theta_n \, d\phi}{I_0} \quad (6)$$

$$I_0 = \int_0^1 \int_0^\pi f'(\theta_p, \theta_i) \, d\cos\theta_n \, d\phi$$

When the substrate is fully covered, this is equivalent to using an averaged value of P_s in Eq. (2) that is

$$\overline{P_s} = 1 - \frac{1}{I_0} \quad (7)$$

The division by I_0 above is also necessary when the substrate is *not* fully covered (i.e. $f_{ex} > 0$), which is often the case for a standard MALDI sample.

For a flat surface, the distribution function f has the form

$$f(\theta_n) = (1 - f_{ex}) \frac{\delta(1 - \cos\theta_n)}{\pi} \quad (8)$$

Here $\delta(x)$ is the delta function and the result above describes crystal surfaces aligned with the substrate. Substitution of this form for $f(\theta_n)$ into the integrals for the averaged yield returns $Y(\cos\theta_p)$. In the following we use values for the distribution of facets having the form

$$f(\theta_n) = (1 - f_{ex}) \frac{(q+2)\cos^q\theta_n}{\pi}, \; q > 0 \quad (9)$$

Again f_{ex} is the fraction of the substrate exposed. Samples described by using the form for $f(\theta_n)$ above have the principal direction of the surface normals perpendicular to the substrate, but the crystallites in the sample have a distribution of normal directions. The larger q is in Eq. (9), the closer the averaged yield approaches that for a flat surface aligned with the substrate. Finally, because $[f(\theta_n)\cos\theta_n]$ is the projection function onto the substrate for normal incidence, $q = 0$ represents an isotropic distribution of facets that is not at all like the samples imaged by Beavis and Brudson [7]. Therefore, q is at least one, but more likely larger than one.

To date there have been no studies of the averaging over the distributions of orientations, even though there have been many studies that purport to describe

the threshold dependence of the yield. If the threshold dependence is a function incident angle, then any threshold dependence on fluence that is reported in the literature is not likely to reflect the true fluence dependence, but is affected by the distribution of surface orientations. Assuming a model for desorption, one should *reanalyze* threshold data using the functions created above to describe the distribution in incident angle to the surfaces of the microcrystals.

Angular distribution of the ejecta

The above results can also be used to estimate the angular distribution of the ejecta from a multifaceted surface. In the absence of crater formation, ablation models typically describe the ejecta leaving perpendicular to the local surface. This is often represented by a large power of the cosine of the ejecta direction giving a steeply forward-peaked distribution [9]. This directionality, we point out, is responsible for producing the crater shape seen for non-normal incidence on a single crystal [10].

Assuming, for simplicity, that the *ejecta leave only along the normal to the local surface*, then the angle of the local ejecta to the substrate normal, described by θ_e and ϕ_e, are equal to the angles describing the surface normal. Now the ejecta distribution from a multifaceted surface can be simplified to

$$\overline{\frac{d^2Y}{d\Omega_e}} \approx \left[\frac{f'(\theta_p,\ \theta_i)Y\ (\cos\ \theta_i)}{I_0}\right]_{\theta_e=\theta_n,\ \phi_e=\phi} \tag{10}$$

Here Ω_e represents the solid angle given by θ_e and ϕ_e. If, instead, a distribution of ejecta angles from each facet is used, then the expression in Eq. (10) would be integrated over such a distribution.

We approximate the incident angular dependence of the yield as

$$Y\ (\cos\ \theta_i) \approx Y_0\ \cos^m\theta_i \tag{11}$$

for the various models for ablation. By using this form and Eq. (9), the molecules ejected exhibit a dependence on the viewing direction written as

$$\frac{d^2Y}{d\Omega_e} \approx \frac{q+2}{2\pi}\frac{Y_0}{I_0\cos\ \theta_p}\left[\cos^q\ \theta_e\ \cos^{m+1}\theta_i\right]_{\theta_i>0}$$

$$\cos\ \theta_i = \cos\ \theta_p \cos\ \theta_e + \sin\ \theta_p \sin\ \theta_e \cos\ \phi_e \tag{12}$$

In this overly simplified result it is seen that the ejecta distribution can exhibit a maximum. Note that if $m = -1$, in which case the yield increases with increasing angle then, quite remarkably, the maximum in yield is perpendicular to the substrate for all incident angles. Of course, such a distribution can apply only over a limited range of angles.

If, as is in the experiments of [3], the viewing direction lies in the plane containing the illumination vector and the surface normal, then the maximum in this distribution is also easily obtained. Whereas in our choice of coordinates θ_e is positive, ϕ_e in the expression for cos θ_i is either π, *away* from direction of illumination so that cos θ_i = cos $(\theta_p + \theta_e)$, or 0, *towards* the direction of illumination giving cos θ_i = cos $(\theta_p - \theta_e)$. By using the latter and differentiating the expression in Eq. (12) one finds the conditions for a maximum in the yield pointed toward the direction of illumination:

$$\tan(\theta_p - \theta_e) = \frac{q}{m+1}\tan\ \theta_e \tag{13}$$

Therefore, the ejecta for *any model* with $m \leq -1$, except, of course, at large angles, *cannot* peak in the backward direction. However, the above does have solutions for values of $m > -1$ and $q > 0$. Therefore, for a variety of models for the incident angle dependence of the yield, the ejecta from a multifaceted surface *can* peak back toward the direction of illumination. That is, the formation of a crater in which the crater walls determine the ejection is *not* necessary to explain the results in [3].

Aksouh et al. [3] found that for an illumination angle, $\theta_p = 60°$, the peak occurs at $\theta_e \approx 30°$, using Eq. (13) models for which $m \approx q - 1$ can describe their result. Unfortunately, there was no characterization of the sample used. However, if the crystal faces in their experiment had a strong orientation parallel to

the substrate, i.e. q large, then the yield would have to be steeply dependent on the angle of incidence in order to obtain their ejecta distribution. Conversely, if the yield for a flat surface is independent angle of incidence (i.e. $m = 0$), the result in [3] will still be obtained if $q = 1$, which may seem surprising. This is discussed below after considering models for MALDI.

Incident angle dependence in MALDI models

Johnson [2] grouped the models for MALDI into a number of classes. In these the yield per pulse for the matrix material, $Y(\cos\theta_i)$, could be written in a general form for a flat surface

$$\begin{aligned} Y(\cos\theta_i) &= n_m \overline{A_p \Delta z}/\cos\theta_i \\ \Delta z(\Phi_p, \theta_i) &= L_c F[\Phi_p \cos\theta_i/\Phi_0] \\ \Phi_0 &\approx c' \frac{n_m U L_c'}{\Delta E_{h\nu}} \end{aligned} \tag{14}$$

Here Y is the total amount of matrix, having molecular number density, n_m, removed by the pulse. The area of the pulse is A_p and incident angle to the flat surface is θ_i. The explicit $\cos\theta_i$ in the first term above accounts for the increase in exposed area with increasing tilt of the beam, as discussed, and the bar indicates an average over the pulse profile. The quantity Δz is the average depth removed in a single shot. Δz is determined in all models by a characteristic length, L_c, and a function, F, which depends on the laser-pulse fluence, Φ_p, as indicated. (In [2] $\Phi_p \cos\theta_i$ was written as Φ). The quantity Φ_0 above is a fluence that is characteristic of the material called the threshold fluence. In all models it is determined, as shown in Eq. (14), by the sublimation energy of the material, U, the amount of the absorbed photon energy released to ablation, $\Delta E_{h\nu}$, and a characteristic length, L_c'. The characteristic lengths L_c and L_c' are determined *either* by the absorbance, α, $[\alpha^{-1} \cos\theta_i]$, which depends explicitly on $\cos\theta_i$ *or* by an energy transport length which is independent of $\cos\theta_i$. *It is the characteristic lengths L_c and L_c' that determine the net dependence of depth removed on the angle of incidence, and, hence, also the dependence of the yield on the angle of incidence.*

The approximate form for the incident angular dependence in Eq. (11) cannot describe the results close to threshold in certain models. A slightly more detailed description is needed and, in any case, the ion threshold fluence is well above the threshold fluence for the matrix. Below, we ignore this problem and give values for m for the various models discussed in [2], labeled A, B, C1, and C2. When low fluence is mentioned, it is a fluence close to the ion threshold and large fluence implies well above the ion threshold.

Although the phrase "thermal model" is used loosely in discussions of MALDI, in models (A) that depend on the molecule by molecule sublimation at the local surface temperature, the prefactor in the expression for Y in Eq. (14) depends inversely on $\cos\theta_i$ and the quantity Δz depends exponentially on $(\cos\theta_i)^{-1}$, except, of course, at large angles. Therefore, at fluences well above the matrix threshold fluence this implies that $m \approx -1$, in which case the results of Aksouh et al. [3] *cannot* be obtained. At low fluences, the yield varies rapidly with fluence and $m \gg 1$ [11,12], so that *if* $q \gg 1$ also (i.e. crystal surfaces very parallel to the substrate), the backward peaking could occur. For the model for laser ablation in which all of the sample is ejected, above that depth at which the energy density deposited is equal to $n_m U$, the yield is independent of the incident angle. Therefore, $m = 0$ at all fluences (model B). As mentioned above, using $m = 0$ gives the observed ejecta distribution for $q \approx 1$, i.e. crystal faces not strongly oriented parallel to the substrate. One might expect that for a yield that is independent of the incident angle, the ejecta direction would *not* vary with incident angle. However, the lack of dependence on angle in the *model* comes about because the thickness, Δz, removed from a flat surface *decreases*, whereas the area exposed *increases* with increasing angle. For a sample of crystal surfaces each much smaller than the beam area, the thickness removed from a microcrystal still changes with incident angle, but increasing the illumination angle relative to the substrate only increases the amount of

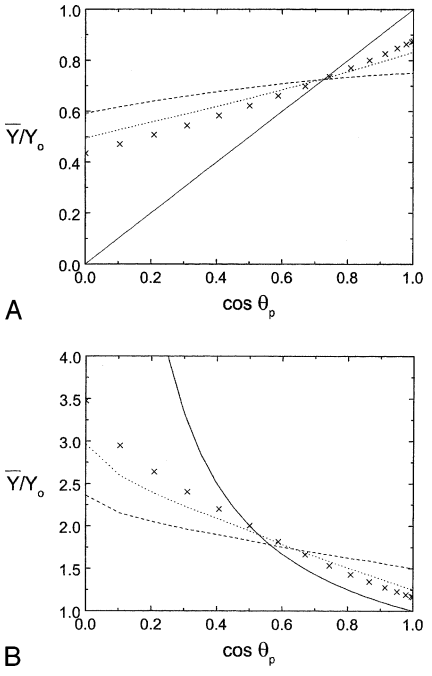

Fig. 1. Average yield assuming a yield that varies as (a) $Y = Y_0 \cos \theta$ and (b) $Y = Y_0/\cos \theta$. The yield is averaged over distributions in surface orientation characterized in Eq. (9) by $q = 0$ (dashed), 1 (dotted), and 2 (crosses). Solid line—no averaging. As q increases, surfaces become increasingly oriented with the substrate and the average yield approaches the solid line.

sample exposed, which clearly does not affect the production into a given direction θ_e.

Finally, two pressure-pulse models were considered [2]. The model called C1 applies in the absence of significant dissipation of the energy deposited by the laser pulse. For model C1, the yield is linear in cos θ_i at low fluences ($m = 1$), but becomes weakly dependent at large fluences and m is small. Therefore, model C1 can account for the measurements *if* $1 < q \approx 2$, with the size of q depending on the fluence. For the pressure-pulse model that includes significant dissipation of the deposited energy, called model C2, the incident angle dependence is described by $m = -1$ over a limited region of applicability of the model (primarily high fluences and not large angles). As discussed above, $m = -1$ *cannot* give the result that is seen near the ion threshold in [3].

In Fig. 1 we give the *yield versus incident angle* averaged over a sample described by Eq. (9) for $q = 1, 2, 3$ for models with $m = 1, -1$ in Eq. (11). It is seen that as q increases, the dependence of the averaged yield approaches that for the flat surface, but the effect of a faceted surface can be considerable. The above results can be used as guidance in interpreting results from a faceted or microcrystalline sample.

Conclusions

We have examined the ablation by a laser pulse of the matrix material used in MALDI experiments. If the sample is formed by vacuum drying of a droplet, it will be composed of crystallites having a distribution in surface orientations; a faceted surface [7]. We have shown how to average the yield over the distribution of crystal faces (surface orientations). This affects the dependence of the yield on angle of incidence (Fig. 1), and averaging should be done when considering the threshold dependence of the yield.

The results, summarized below, were obtained by assuming that the ejecta leave roughly perpendicular to the local surface when working close to "threshold." This is a reasonable assumption as the surface area exposed is generally large compared to the thickness removed in a single shot near threshold. In fact, following the exposure of a sample to a large number of laser pulses incident at 45° onto a uniform MALDI matrix, the exposed surface in the crater becomes nearly perpendicular to the beam direction [10]. Therefore, when a crater *does* develop, the observed backward-directed ejecta will come about naturally and not due to the redirection of the ejecta by scattering off the walls of the crater [6]. The crater evolves in the manner observed in [10] because the laser pulse has a radial profile *and* the geometry for non-normal incidence causes the maximum depth removed to be shifted forward from the center of the pulse. Therefore, averaging over the radial profile is necessary to describe the effect [13].

By using an analytic form for the distribution of crystal-face orientations, we showed in this article that averaging the yield over the distribution of

orientations is important. In particular, the ejecta distribution is significantly modified by the surface-orientation distribution and depends on the angular distribution of the yield. Averaging over model distributions we showed that the result of Aksouh et al. [3] can be obtained *without* assuming that the crater walls determine the direction of the ejecta. We also pointed out that the measured angular distribution of the ejecta can be used to help discriminate among the proposed models, especially if the distribution of surfaces orientations is known. In the experiments in [3] the ejecta was directed backward toward the illumination direction: an angle of ~30° to the substrate normal for an illumination angle of ~60° to the subtrate normal. Although the surface was *not* characterized, such a result can be obtained for certain "thermal" models (models A in [2]) near threshold *if* the crystal surface normals have a *strong* correlation with the substrate normal. Conversely, the models labeled B and C1 in [2] *are* able to give this result only if the surface normals have a *weak* correlation with the subtrate normal, a cosine dependence for B and up to cosine squared for C1. Experiments like those in [3] are now needed for samples that are well characterized and for low fluence.

Acknowledgements

The authors acknowledge helpful comments from R. Beavis and B. Chait. This work was supported in part by a grant from the French CNRS for a visit to Orsay by REJ in July 1997 and in part by an NSF grant.

Appendix

To calculate the distribution function and verify the averaging of Y we consider an exposed surface made up of small surfaces with area ΔA_n, where n is the direction of the normal to the local surface. For normal incidence to the substrate, full coverage of the substrate, and pulse area A_p,

$$\Sigma_{\mathrm{ex}}\, \Delta A_n \cos\,\theta_n = A_p \tag{A1}$$

The subscript ex implies the sum is over exposed surfaces. For an illumination angle by the laser to the substrate normal of θ_p,

$$\Sigma'_{\mathrm{ex}}\, \Delta A_n \cos\,\theta_i = A_p \tag{A2}$$

$$\cos\,\theta_i = \cos\,\theta_p \cos\,\theta_n + \sin\,\theta_p \sin\,\theta_n \cos\,\phi$$

Here the prime indicates that the sum over microcrystal surfaces is extended over a larger substrate area because of the illumination angle. Defining

$$f(\theta_n) \approx \frac{\Sigma^{(n)} \Delta A_n}{A_p} \tag{A3}$$

where the sum now is over all facets on the surface that have the direction θ_n. Now changing the sum of exposed surfaces in Eq. (A1) to an integral, the result in Eq. (1) is obtained. If the same amount of surface in Eq. (A2) is summed over as was the case in Eq. (A1) then, instead of the prime, we could write Eq. (A2) as

$$\frac{1}{\cos\,\theta_p}\, \Sigma_{\mathrm{ex}} \Delta A_n \cos\,\theta_i = A_p$$

Again, replacing the sum by an integral, the distribution function in Eq. (2) is obtained. That is,

$$\frac{\Sigma_{\mathrm{ex}} \Delta A_n}{A_p \cos\,\theta_p} \approx \int_{\mathrm{ex}} \int_{\mathrm{ex}} f(\theta_n,\, \theta_p)\, d\cos\,\theta_n\, d\phi$$

$$= \int_{\mathrm{ex}} \int_{\mathrm{ex}} \frac{1}{\cos\,\theta_p} f(\theta_n) \cos\,\theta_i\, d\cos\,\theta_n\, d\phi \tag{A4}$$

so that

$$f(\theta_n,\, \theta_p) = \left(\frac{1}{\cos\,\theta_p} f(\theta_n) \cos\,\theta_i \right)_{\mathrm{ex}}$$

$$= \frac{1}{\cos\,\theta_p} f(\theta_n) \cos\,\theta_i\, \Theta(\cos\,\theta_i)$$

$$\times [1 - P_s(\theta_n,\, \theta_p)]$$

giving the results in Eqs. (2) and (4).

The form for the yield in Eq. (14) suggests how to obtain the contribution to the yield,

$$\Delta Y_n = n_m \Delta A_n \Delta z(\Phi_p, \theta_i) \tag{A5}$$

from a microsurface that has an area much smaller than the beam area. Here the only angular dependence is in the thickness removed and is indicated explicitly. The average yield is now obtained by summing over all surfaces exposed, i.e. all contributions to the yield,

$$\overline{Y(\cos\theta_p)} \approx \Sigma'_{\mathrm{ex}}\ \Delta Y_n \approx \frac{1}{\cos\theta_p}\Sigma_{\mathrm{ex}}\Delta Y_n \tag{A6}$$

By using the results above and replacing the sum by an integration over surface normal directions, this can be written in the form

$$\overline{Y(\cos\theta_p)} = \frac{n_m A_p}{\cos\theta_p} \times \int_{\mathrm{ex}}\int_{\mathrm{ex}} f(\theta_n)\Delta z(\cos\theta_i)\, d\cos\theta_n\, d\phi \tag{A7}$$

This expression may be more transparent than the ones in the text. It states that the contribution to the yield comes from all of the surfaces exposed to the beam with a given angle. Each such surface loses the same thickness of material, Δz. However, the yield is typically defined as in Eq. (14), i.e. as the volume removed and not the thickness removed. Therefore, by using the form for Y in Eq. (14), the result in Eq. (5) is obtained. Note that the overbar on the right of the first expression in Eq. (14) implies that the beam is typically not spatially uniform, which was ignored in the discussion above.

References

[1] F. Hillenkamp, M. Karas, R.C. Beavis, B.T. Chait, Anal. Chem. 63 (1991) 1193A.
[2] R.E. Johnson, in Large Ions: Their Vaporization, Detection, and Structural Analysis, T. Baer, C.-Y. Ng, I. Powis (Eds.), Wiley, Chichester, 1996, p. 49.
[3] P. Aksouh, P. Chaurand, C. Deprun, S. Della-Negra, J. Hoyes, Y. LeBeyec, R. Rosas Pinho, Rapid Commun. Mass Spectrom. 9 (1995) 515.
[4] A. Brunelle, S. Della-Negra, Y. LeBeyec, Nucl. Instrum. Methods Phys. Res. B 132 (1997) 718.
[5] R.M. Papaléo, P. Demirev, J. Eirksson, P. Håkansson, B.U.R. Sundqvist, R.E. Johnson, Phys. Rev. Lett. 77 (1996) 667.
[6] V. Bokelmann, B. Spengler, R. Kaufmann, Eur. Mass Spectrom. 1 (1995) 81.
[7] R.C. Beavis, J.N. Bridson, J. Phys. D, 26 (1993) 442.
[8] A. Westmann, T. Huth-Fehre, P. Demirev, J. Bielawski, N. Medina, B.U.R. Sundqvist, Rapid Commun. Mass Spectrom. 8 (1994) 388.
[9] W. Zhang and B.T. Chait, Int. J. Mass Spectrom. Ion Processes 160 (1997) 259.
[10] I. Fournier, R.C. Beavis, J.C. Blais, J.C. Tabet, G. Bolbach, Int. J. Mass Spectrom. Ion Phys. 169/170 (1998) 19.
[11] K. Dreisewerd, M. Schorenberg, M. Karas, F. Hillenkamp, Int. J. Mass Spectrom. Ion Processes 141 (1995) 127.
[12] M. Karas, U. Bahr, and J.-R. Stahl-Zeng, in Large Ions: Their Vaporization, Detection and Structural Analysis, T. Baer, C.-Y. Ng, I. Powis (Eds.), Wiley, Chichester, 1996, p. 27.
[13] R.C. Beavis, Org. Mass Spectrom. 27 (1992) 864.